University of Gloucestershire
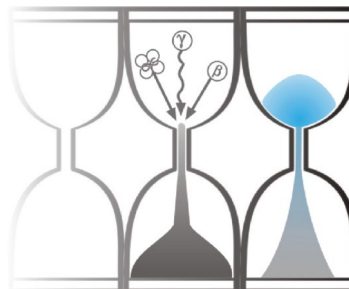
Geochronology Laboratories

Optical dating of sediments, Steart Point, UK

to

J. Russell, Wessex Archaeology

Prepared by Dr P.S. Toms, 12 March 2012

Contents

Scope of Report

This is a standard report of the Geochronology Laboratories, University of Gloucestershire. In large part, the document summarises the processes, diagnostics and data drawn upon to deliver Table 1. A conclusion on the analytical validity of each sample's optical age estimate is expressed in Table 2; where there are caveats, the reader is directed to the relevant section of the report that explains the issue further in general terms.

Field Code	Lab Code	Overburden (m)	Grain size (µm)	Moisture content (%)	NaI γ-spectrometry (in situ)			$\gamma\ D_r$ (Gy.ka^{-1})	Ge γ-spectrometry (lab based)			$\alpha\ D_r$ (Gy.ka^{-1})	$\beta\ D_r$ (Gy.ka^{-1})	Cosmic D_r (Gy.ka^{-1})	Total D_r (Gy.ka^{-1})	Preheat (°C for 10s)	Low Dose Repeat Ratio	High Dose Repeat Ratio	Post-IR OSL Ratio	D_e (Gy)	Age (ka)
					K (%)	Th (ppm)	U (ppm)		K (%)	Th (ppm)	U (ppm)										
BH105 7.80-8.25m	GL11022	7.98	125-180	30 ± 7	-	-	-	0.60 ± 0.09	1.38 ± 0.06	7.79 ± 0.50	1.57 ± 0.09	-	0.91 ± 0.13	0.06 ± 0.01	1.57 ± 0.19	250	0.99 ± 0.03	0.99 ± 0.01	0.99 ± 0.02	1.9 ± 0.1	1.2 ± 0.2 (0.2)
BH102 10.00-10.45m	GL11023	10.20	5-15	23 ± 6	-	-	-	1.16 ± 0.11	2.12 ± 0.09	8.73 ± 0.54	5.46 ± 0.23	0.60 ± 0.07	1.97 ± 0.21	0.05 ± 0.01	3.78 ± 0.25	260	0.98 ± 0.16	0.90 ± 0.12	0.90 ± 0.21	687.3 ± 110.9	169 ± 31 (31)

Table 1 D_r, D_e and Age data of submitted samples located at c. 51°N, 3°W, 7 m. Ages expressed relative to year of sampling. Uncertainties in age are quoted at 1σ confidence, are based on analytical errors and reflect combined systematic and experimental variability and (in parenthesis) experimental variability alone (see 6.0). Blue indicates samples with accepted age estimates, red, age estimates with caveats (see Table 2).

Generic considerations	Field Code	Lab Code	Sample specific considerations
Absence of *in situ* γ spectrometry data (see 4.0)	BH105 7.80-8.25m	GL11022	None
	BH102 10.00-10.45m	GL11023	D_e exceeds functional range (see 3.1.3, Table 1) Natural signal in 43% of aliquots equivalent to saturation Accept tentatively as minimum age

Table 2 Analytical validity of sample suite age estimates and caveats for consideration

1.0 Mechanisms and principles

Upon exposure to ionising radiation, electrons within the crystal lattice of insulating minerals are displaced from their atomic orbits. Whilst this dislocation is momentary for most electrons, a portion of charge is redistributed to meta-stable sites (traps) within the crystal lattice. In the absence of significant optical and thermal stimuli, this charge can be stored for extensive periods. The quantity of charge relocation and storage relates to the magnitude and period of irradiation. When the lattice is optically or thermally stimulated, charge is evicted from traps and may return to a vacant orbit position (hole). Upon recombination with a hole, an electron's energy can be dissipated in the form of light generating crystal luminescence providing a measure of dose absorption.

Herein, quartz is segregated for dating. The utility of this minerogenic dosimeter lies in the stability of its datable signal over the mid to late Quaternary period, predicted through isothermal decay studies (e.g. Smith *et al.*, 1990; retention lifetime 630 Ma at 20°C) and evidenced by optical age estimates concordant with independent chronological controls (e.g. Murray and Olley, 2002). This stability is in contrast to the anomalous fading of comparable signals commonly observed for other ubiquitous sedimentary minerals such as feldspar and zircon (Wintle, 1973; Templer, 1985; Spooner, 1993)

Optical age estimates of sedimentation (Huntley *et al.*, 1985) are premised upon reduction of the minerogenic time dependent signal (Optically Stimulated Luminescence, OSL) to zero through exposure to sunlight and, once buried, signal reformulation by absorption of litho- and cosmogenic radiation. The signal accumulated post burial acts as a dosimeter recording total dose absorption, converting to a chronometer by estimating the rate of dose absorption quantified through the assay of radioactivity in the surrounding lithology and streaming from the cosmos.

$$\text{Age} = \frac{\text{Mean Equivalent Dose } (D_e, \text{Gy})}{\text{Mean Dose Rate } (D_r, \text{Gy.ka}^{-1})}$$

Aitken (1998) and Bøtter-Jensen et al. (2003) offer a detailed review of optical dating.

2.0 Sample Preparation

A total of four sediment samples were submitted from two vibrocores for Optical dating (Table 1). The cores were bisected in daylight to identify the apposite sampling position in consultation with J. Russell, Wessex Archaeology. To preclude optical erosion of the datable signal prior to measurement both lengths of each core were moved into and prepared under controlled laboratory illumination, provided by Encapsulite RB-10 (red) filters. Sediment exposed to daylight during bisection was removed from each sample position to a depth of 10 mm from each bisected face. The remaining sediment was then sectioned into a 50-100 mm length (depending on unit thickness), 40 mm wide sample using aluminium separators to preclude incorporation of material transferred down the core walls during retrieval. Sub-samples of c. 50 g were taken from within each position to establish D_r values.

Each dating sample was then weighed, dried, reweighed and sieved. For sample GL11022 quartz within the fine sand (125-180 µm) fraction was segregated, whilst for sample GL11023 fine silt (5-15 µm) was pursued (Table 1). Samples were then subjected to acid and alkaline digestion (10% HCl, 15% H_2O_2) to attain removal of carbonate and organic components respectively.

For GL11022, a further acid digestion in HF (40%, 60) was used to etch the outer 10-15 µm layer affected by α radiation and degrade each samples' feldspar content. During HF treatment, continuous magnetic stirring was used to effect isotropic etching of grains. 10% HCl was then added to remove acid soluble fluorides. The sample was dried, resieved

and quartz isolated from the remaining heavy mineral fraction using a sodium polytungstate density separation at 2.68g.cm^{-3}. 12 multi-grain aliquots (*c.* 3-6 mg) of quartz from the sample were then mounted on aluminium discs for determination of D_e values.

For GL11023 fine silt sized quartz, along with other mineral grains of varying density and size, was extracted by sedimentation in acetone (<15 μm in 2 min 20 s, >5 μm in 21 mins at 20ºC). Feldspars and amorphous silica were then removed from this fraction through acid digestion (35% H_2SiF_6 for 2 weeks, Jackson *et al.*, 1976; Berger *et al.*, 1980). Following addition of 10% HCl to remove acid soluble fluorides, grains degraded to <5 μm as a result of acid treatment were removed by acetone sedimentation. 7 aliquots (ca. 1.5 mg) were then mounted on aluminium discs for D_e evaluation.

All drying was conducted at 40°C to prevent thermal erosion of the signal. All acids and alkalis were Analar grade. All dilutions (removing toxic-corrosive and non-minerogenic luminescence-bearing substances) were conducted with distilled water to prevent signal contamination by extraneous particles.

3.0 Acquisition and accuracy of D_e value

All minerals naturally exhibit marked inter-sample variability in luminescence per unit dose (sensitivity). Therefore, the estimation of D_e acquired since burial requires calibration of the natural signal using known amounts of laboratory dose. D_e values were quantified using a single-aliquot regenerative-dose (SAR) protocol (Murray and Wintle 2000; 2003) facilitated by a Risø TL-DA-15 irradiation-stimulation-detection system (Markey *et al.*, 1997; Bøtter-Jensen *et al.*, 1999). Within this apparatus, optical signal stimulation is provided by a 150 W tungsten halogen lamp, filtered to a broad blue-green light, 420-560 nm (2.21-2.95 eV) conveying 16 mWcm^{-2}, using three 2 mm Schott GG420 and a broadband interference filter. Infrared (IR) stimulation, provided by 6 IR diodes (Telefunken TSHA 6203) stimulating at 875±80nm delivering ~5 mW.cm^{-2}, was used to indicate the presence of contaminant feldspars (Hütt *et al.*, 1988). Stimulated photon emissions from quartz aliquots are in the ultraviolet (UV) range and were filtered from stimulating photons by 7.5 mm HOYA U-340 glass and detected by an EMI 9235QA photomultiplier fitted with a blue-green sensitive bialkali photocathode. Aliquot irradiation was conducted using a 1.48 GBq ^{90}Sr/^{90}Y β source calibrated for multi-grain aliquots of each isolated quartz fraction against the 'Hotspot 800' ^{60}Co γ source located at the National Physical Laboratory (NPL), UK.

SAR by definition evaluates D_e through measuring the natural signal (Fig. 1) of a single aliquot and then regenerating that aliquot's signal by using known laboratory doses to enable calibration. For each aliquot, 5 different regenerative-doses were administered so as to image dose response. D_e values for each aliquot were then interpolated, and associated counting and fitting errors calculated, by way of exponential plus linear regression (Fig. 1). Weighted (geometric) mean D_e values were calculated using the central age model outlined by Galbraith *et al.* (1999) and are quoted at 1σ confidence. The accuracy with which D_e equates to total absorbed dose and that dose absorbed since burial was assessed. The former can be considered a function of laboratory factors, the latter, one of environmental issues. Diagnostics were deployed to estimate the influence of these factors and criteria instituted to optimise the accuracy of D_e values.

3.1 Laboratory Factors

3.1.1 Feldspar contamination

The propensity of feldspar signals to fade and underestimate age, coupled with their higher sensitivity relative to quartz makes it imperative to quantify feldspar contamination. At room temperature, feldspars generate a signal (IRSL) upon exposure to IR whereas quartz does not. The signal from feldspars contributing to OSL can be depleted by prior exposure to IR. For all aliquots the contribution of any remaining feldspars was estimated from the OSL IR depletion ratio

(Duller, 2003). If the addition to OSL by feldspars is insignificant, then the repeat dose ratio of OSL to post-IR OSL should be statistically consistent with unity (Figs 1 and Fig. 5; Table 1). If any aliquots do not fulfil this criterion, then the sample age estimate should be accepted tentatively. The source of feldspar contamination is rarely rooted in sample preparation; it predominantly results from the occurrence of feldspars as inclusions within quartz.

3.1.2 Preheating

Preheating aliquots between irradiation and optical stimulation is necessary to ensure comparability between natural and laboratory-induced signals. However, the multiple irradiation and preheating steps that are required to define single-aliquot regenerative-dose response leads to signal sensitisation, rendering calibration of the natural signal inaccurate. The SAR protocol (Murray and Wintle, 2000; 2003) enables this sensitisation to be monitored and corrected using a test dose to track signal sensitivity between irradiation-preheat steps. The test dose for GL11022 was set at 5 Gy, preheated to 220°C for 10s. Owing to insensitivity of OSL within sample GL11023, the test dose was set at 20 Gy.

The accuracy of sensitisation correction for both natural and laboratory signals can be preheat dependent. The Dose Recovery test was used to assess the optimal preheat temperature for accurate correction and calibration of the time dependent signal. Dose Recovery (Fig. 2) attempts to quantify the combined effects of thermal transfer and sensitisation on the natural signal, using a precise lab dose to simulate natural dose. The ratio between the applied dose and recovered D_e value should be statistically concordant with unity. For this diagnostic, 6 aliquots were each assigned a 10 s preheat between 180°C and 280°C.

That preheat treatment fulfilling the criterion of accuracy within the Dose Recovery test was selected to generate the final D_e value. Further thermal treatments, prescribed by Murray and Wintle (2000; 2003), were applied to optimise accuracy and precision. Optical stimulation occurred at 125ºC in order to minimise effects associated with photo-transferred thermoluminescence and maximise signal to noise ratios. Inter-cycle optical stimulation was conducted at 280ºC to minimise recuperation.

3.1.3 Irradiation

For all samples having D_e values in excess of 100 Gy, matters of signal saturation and laboratory irradiation effects are of concern. With regards the former, the rate of signal accumulation generally adheres to a saturating exponential form and it is this that limits the precision and accuracy of D_e values for samples having absorbed large doses. For such samples, the functional range of D_e interpolation by SAR has been verified up to 600 Gy by Pawley *et al.* (2010). Age estimates based on D_e values exceeding this value should be accepted tentatively.

3.1.4 Internal consistency

Quasi-radial plots (*cf* Galbraith, 1990) are used to illustrate inter-aliquot D_e variability for natural, repeat regenerative-dose and OSL to post-IR OSL signals (Figs 3 to 5, respectively; Table 1). D_e values are standardised relative to the central D_e value for natural signals and applied dose for regenerated signals. D_e values are described as overdispersed when >5% lie beyond $\pm 2\sigma$ of the standardising value; resulting from a heterogeneous absorption of burial dose and/or response to the SAR protocol. For multi-grain aliquots, overdispersion of natural signals does not necessarily imply inaccuracy. However where overdispersion is observed for regenerated signals, the efficacy of sensitivity correction may be problematic. This measure of SAR protocol success at Gloucestershire differs and is more stringent than that prescribed by Murray and Wintle (2000; 2003). They suggest repeat dose ratios (Table 1) should be concordant with the range 0.9-1.1; this filter of analytical validity has been applied in this study (Table 2).

3.2 Environmental factors

3.2.1 Incomplete zeroing

Post-burial OSL signals residual of pre-burial dose absorption can result where pre-burial sunlight exposure is limited in spectrum, intensity and/or period, leading to age overestimation. This effect is particularly acute for material eroded and redeposited sub-aqueously (Olley *et al.*, 1998, 1999; Wallinga, 2002) and exposed to a burial dose of <20 Gy (e.g. Olley *et al.*, 2004), has some influence in sub-aerial contexts but is rarely of consequence where aerial transport has occurred. Within single-aliquot regenerative-dose optical dating there are two diagnostics of partial resetting (or bleaching); signal analysis (Agersnap-Larsen *et al.*, 2000; Bailey *et al.*, 2003) and inter-aliquot D_e distribution studies (Murray *et al.*, 1995).

Within this study, signal analysis was used to quantify the change in D_e value with respect to optical stimulation time for multi-grain aliquots. This exploits the existence of traps within minerogenic dosimeters that bleach with different efficiency for a given wavelength of light to verify partial bleaching. D_e (t) plots (Fig. 6; Bailey *et al.*, 2003) are constructed from separate integrals of signal decay as laboratory optical stimulation progresses. A statistically significant increase in natural D_e (t) is indicative of partial bleaching assuming three conditions are fulfilled. Firstly, that a statistically significant increase in D_e (t) is observed when partial bleaching is simulated within the laboratory. Secondly, that there is no significant rise in D_e (t) when full bleaching is simulated. Finally, there should be no significant augmentation in D_e (t) when zero dose is simulated. Where partial bleaching is detected, the age derived from the sample should be considered a maximum estimate only. However, the utility of signal analysis is strongly dependent upon a samples pre-burial experience of sunlight's spectrum and its residual to post-burial signal ratio. Given in the majority of cases, the spectral exposure history of a deposit is uncertain, the absence of an increase in natural D_e (t) does not necessarily testify to the absence of partial bleaching.

Where requested and feasible, the insensitivities of multi-grain single-aliquot signal analysis may be circumvented by inter-aliquot D_e distribution studies. This analysis uses aliquots of single sand grains to quantify inter-grain D_e distribution. At present, it is contended that asymmetric inter-grain D_e distributions are symptomatic of partial bleaching and/or pedoturbation (Murray *et al.*, 1995; Olley *et al.*, 1999; Olley *et al.*, 2004; Bateman *et al.*, 2003). For partial bleaching at least, it is further contended that the D_e acquired during burial is located in the minimum region of such ranges. The mean and breadth of this minimum region is the subject of current debate, as it is additionally influenced by heterogeneity in microdosimetry, variable inter-grain response to SAR and residual to post-burial signal ratios. Presently, the apposite measure of age is that defined by the D_e interval delimited by the minimum and central age models of Galbraith *et al.* (1999).

3.2.2 Pedoturbation

The accuracy of sedimentation ages can further be controlled by post-burial trans-strata grain movements forced by pedo- or cryoturbation. Berger (2003) contends pedogenesis prompts a reduction in the apparent sedimentation age of parent material through bioturbation and illuviation of younger material from above and/or by biological recycling and resetting of the datable signal of surface material. Berger (2003) proposes that the chronological products of this remobilisation are A-horizon age estimates reflecting the cessation of pedogenic activity, Bc/C-horizon ages delimiting the maximum age for the initiation of pedogenesis with estimates obtained from Bt-horizons providing an intermediate age 'close to the age of cessation of soil development'. Singhvi et al. (2001), in contrast, suggest that B and C-horizons closely approximate the age of the parent material, the A-horizon, that of the 'soil forming episode'. At present there is no post-sampling mechanism for the direct detection of and correction for post-burial sediment remobilisation. However, intervals of palaeosol evolution can be delimited by a maximum age derived from parent material and a minimum age obtained from a unit overlying the palaeosol. Inaccuracy forced by cryoturbation may be bidirectional, heaving older material upwards or drawing younger material downwards into the level to be dated. Cryogenic deformation of matrix-supported material is, typically, visible; sampling of such cryogenically-disturbed sediments can be avoided.

4.0 Acquisition and accuracy of D_r value

Lithogenic D_r values were defined through measurement of U, Th and K radionuclide concentration and conversion of these quantities into α, β and γ D_r values (Table 1). α and β contributions were estimated from sub-samples by laboratory-based γ spectrometry using an Ortec GEM-S high purity Ge coaxial detector system, calibrated using certified reference materials supplied CANMET. γ dose rates can be estimated from *in situ* NaI gamma spectrometry to reduce uncertainty relating to potential heterogeneity in the γ dose field surrounding each sample. Where direct measurements are unavailable as in the present case, laboratory-based Ge γ spectrometry can be used to profile the γ field at intervals within 300 mm above and below of each sample's centre. However, core section length in this study precluded profiling. The level of U disequilibrium was estimated by laboratory-based Ge γ spectrometry. Estimates of radionuclide concentration were converted into D_r values (Adamiec and Aitken, 1998), accounting for D_r modulation forced by grain size (Mejdahl, 1979), present moisture content (Zimmerman, 1971) and, where D_e values were generated from 5-15 μm quartz, reduced signal sensitivity to α radiation (a-value 0.050 ± 0.002; Toms, unpub. data). Cosmogenic D_r values were calculated on the basis of sample depth, geographical position and matrix density (Prescott and Hutton, 1994).

The spatiotemporal validity of D_r values can be considered a function of five variables. Firstly, age estimates devoid of *in situ* γ spectrometry data should be accepted tentatively if the sampled unit is heterogeneous in texture or if the sample is located within 300 mm of strata consisting of differing texture and/or mineralogy. However, where samples are obtained throughout a vertical profile, consistent values of γ D_r based solely on laboratory measurements may evidence the homogeneity of the γ field and hence accuracy of γ D_r values. Secondly, disequilibrium can force temporal instability in U and Th emissions. The impact of this infrequent phenomenon (Olley et al., 1996) upon age estimates is usually insignificant given their associated margins of error. However, for samples where this effect is pronounced (>50% disequilibrium between ^{238}U and ^{226}Ra; Fig. 7), the resulting age estimates should be accepted tentatively. Thirdly, pedogenically-induced variations in matrix composition of B and C-horizons, such as radionuclide and/or mineral remobilisation, may alter the rate of energy emission and/or absorption. If D_r is invariant through a dated profile and samples encompass primary parent material, then element mobility is likely limited in effect. Fourthly, spatiotemporal detractions from present moisture content are difficult to assess directly, requiring knowledge of the magnitude and timing of differing contents. However, the maximum influence of moisture content variations can be delimited by recalculating D_r for minimum (zero) and maximum (saturation) content. Finally, temporal alteration in the thickness of overburden alters cosmic D_r values. Cosmic D_r often forms a negligible portion of total D_r. It is possible to quantify the maximum influence of overburden flux by recalculating D_r for minimum (zero) and maximum (surface sample) cosmic D_r.

5.0 Estimation of Age

Age estimates reported in Table 1 provide an estimate of sediment burial period based on mean D_e and D_r values and their associated analytical uncertainties. Uncertainty in age estimates is reported as a product of systematic and experimental errors, with the magnitude of experimental errors alone shown in parenthesis (Table 1). Probability distributions indicate the inter-aliquot variability in age (Fig. 8). The maximum influence of temporal variations in D_r forced by minima-maxima in moisture content and overburden thickness is illustrated in Fig. 8. Where uncertainty in these parameters exists this age range may prove instructive, however the combined extremes represented should not be construed as preferred age estimates. The analytical validity of each sample is presented in Table 2.

6.0 Analytical uncertainty

All errors are based upon analytical uncertainty and quoted at 1σ confidence. Error calculations account for the propagation of systematic and/or experimental (random) errors associated with D_e and D_r values.

For D_e values, systematic errors are confined to laboratory β source calibration. Uncertainty in this respect is that combined from the delivery of the calibrating γ dose (1.2%; NPL, pers. comm.), the conversion of this dose for SiO_2 using the respective mass energy-absorption coefficient (2%; Hubbell, 1982) and experimental error, totalling 3.5%. Mass attenuation and bremsstrahlung losses during γ dose delivery are considered negligible. Experimental errors relate to D_e interpolation using sensitisation corrected dose responses. Natural and regenerated sensitisation corrected dose points (S_i) were quantified by,

$$S_i = (D_i - x.L_i) / (d_i - x.L_i)$$ **Eq.1**

where $D_i =$ Natural or regenerated OSL, initial 0.2 s
       $L_i =$ Background natural or regenerated OSL, final 5 s
       $d_i =$ Test dose OSL, initial 0.2 s
       $x =$ Scaling factor, 0.08

The error on each signal parameter is based on counting statistics, reflected by the square-root of measured values. The propagation of these errors within Eq. 1 generating σS_i follows the general formula given in Eq. 2. σS_i were then used to define fitting and interpolation errors within exponential plus linear regressions.

For D_r values, systematic errors accommodate uncertainty in radionuclide conversion factors (5%), β attenuation coefficients (5%), a-value (4%; derived from a systematic α source uncertainty of 3.5% and experimental error), matrix density (0.20 $g.cm^{-3}$), vertical thickness of sampled section (specific to sample collection device), saturation moisture content (3%), moisture content attenuation (2%), burial moisture content (25% relative, unless direct evidence exists of the magnitude and period of differing content) and NaI gamma spectrometer calibration (3%). Experimental errors are associated with radionuclide quantification for each sample by NaI and Ge gamma spectrometry.

The propagation of these errors through to age calculation was quantified using the expression,

$$\sigma y \ (\delta y/\delta x) = (\Sigma \ ((\delta y/\delta x_n).\sigma x_n)^2)^{1/2}$$ **Eq. 2**

where y is a value equivalent to that function comprising terms x_n and where σy and σx_n are associated uncertainties.

Errors on age estimates are presented as combined systematic and experimental errors and experimental errors alone. The former (combined) error should be considered when comparing luminescence ages herein with independent chronometric controls. The latter assumes systematic errors are common to luminescence age estimates generated by means identical to those detailed herein and enable direct comparison with those estimates.
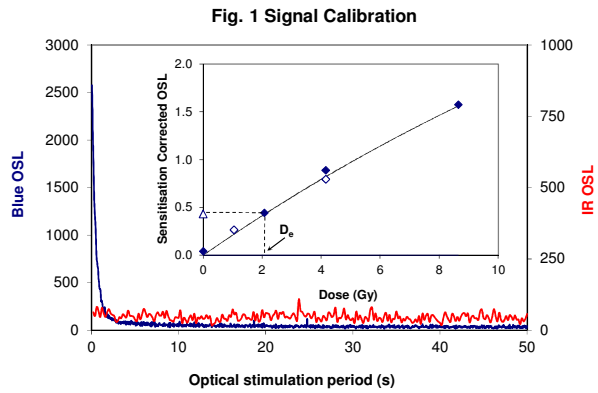
Fig. 1 Signal Calibration

Fig. 2 Dose Recovery

Fig. 6 Signal Analysis

Fig. 3 Inter-aliquot D$_e$ distribution

Fig. 4 Low and High Repeat Regenerative-dose Ratio

Fig. 7 U Decay Activity

Fig. 5 OSL to Post-IR OSL Ratio

Fig. 8 Age Range

Fig. 1 Signal Calibration Natural blue and laboratory-induced infrared (IR) OSL signals. Detectable IR signal decays are diagnostic of feldspar contamination. Inset, the natural blue OSL signal (open triangle) of each aliquot is calibrated against known laboratory doses to yield equivalent dose (D$_e$) values. Repeats of low and high doses (open diamonds) illustrate the success of sensitivity correction.

Fig. 2 Dose Recovery The acquisition of D$_e$ values is necessarily predicated upon thermal treatment of aliquots succeeding environmental and laboratory irradiation. The Dose Recovery test quantifies the combined effects of thermal transfer and sensitisation on the natural signal using a precise lab dose to simulate natural dose. Based on this an appropriate thermal treatment is selected to generate the final D$_e$ value.

Fig. 3 Inter-aliquot D$_e$ distribution Provides a measure of inter-aliquot statistical concordance in D$_e$ values derived from **natural** irradiation. Discordant data (those points lying beyond ±2 standardised ln D$_e$) reflects heterogeneous dose absorption and/or inaccuracies in calibration.

Fig. 4 Low and High Repeat Regenerative-dose Ratio Measures the statistical concordance of signals from repeated **low** and **high** regenerative-doses. Discordant data (those points lying beyond ±2 standardised ln D$_e$) indicate inaccurate sensitivity correction.

Fig. 5 OSL to Post-IR OSL Ratio Measures the statistical concordance of OSL and post-IR OSL responses to the same regenerative-dose. Discordant, underestimating data (those points lying below -2 standardised ln D$_e$) highlight the presence of significant feldspar contamination.

Fig. 6 Signal Analysis Statistically significant increase in **natural** D$_e$ value with signal stimulation period is indicative of a partially-bleached signal, provided a significant increase in D$_e$ results from **simulated partial bleaching** followed by insignificant adjustment in D$_e$ for simulated **zero** and **full bleach** conditions. Ages from such samples are considered maximum estimates. In the absence of a significant rise in D$_e$ with stimulation time, simulated partial bleaching and zero/full bleach tests are not assessed.

Fig. 7 U Activity Statistical concordance (equilibrium) in the activities of the daughter radioisotope ^{226}Ra with its parent ^{238}U may signify the temporal stability of D$_r$ emissions from these chains. Significant differences (disequilibrium; >50%) in activity indicate addition or removal of isotopes creating a time-dependent shift in D$_r$ values and increased uncertainty in the accuracy of age estimates. A 20% disequilibrium marker is also shown.

Fig. 8 Age Range The **mean age range** provides an estimate of sediment burial period based on mean D$_e$ and D$_r$ values with associated analytical uncertainties. The probability distribution indicates the inter-aliquot variability in age. The maximum influence of temporal variations in D$_r$ forced by minima-maxima variation in moisture content and overburden thickness may prove instructive where there is uncertainty in these parameters, however the combined extremes represented should not be construed as preferred age estimates.
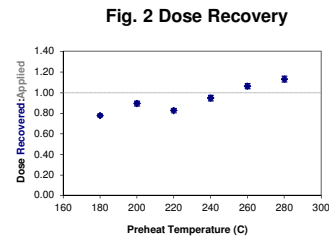
Sample: GL11022

Fig. 1 Signal Calibration
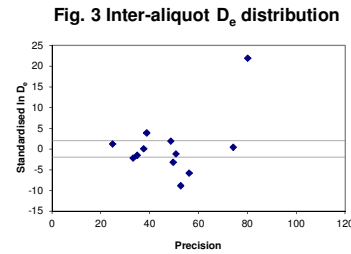

Fig. 2 Dose Recovery

Fig. 3 Inter-aliquot D_e distribution

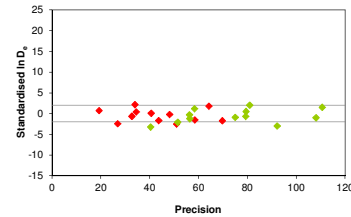## Fig. 4 Low and High Repeat Regenerative-dose Ratio
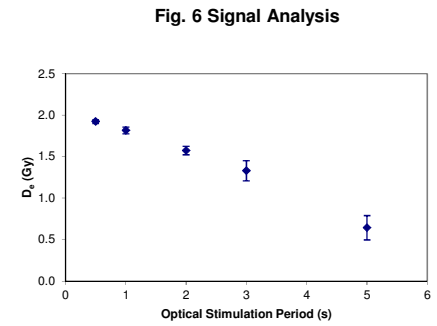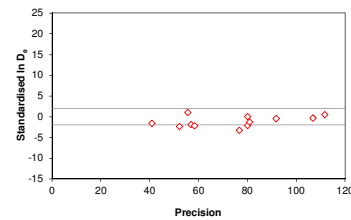

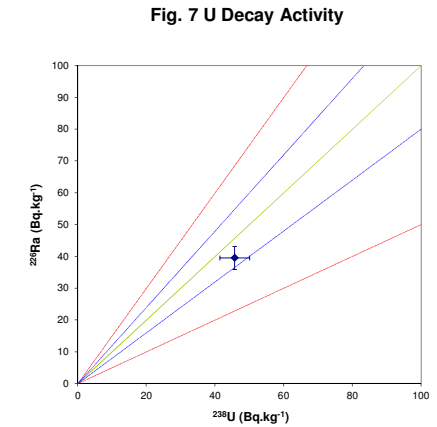## Fig. 5 OSL to Post-IR OSL Ratio

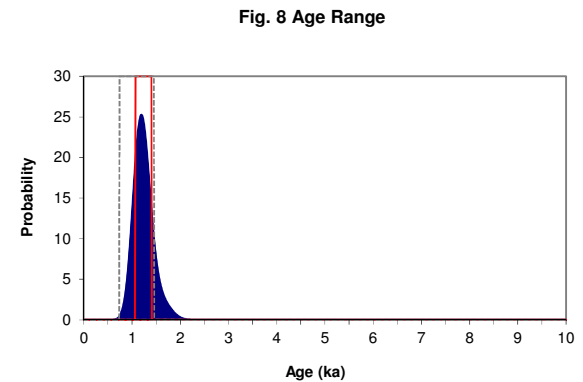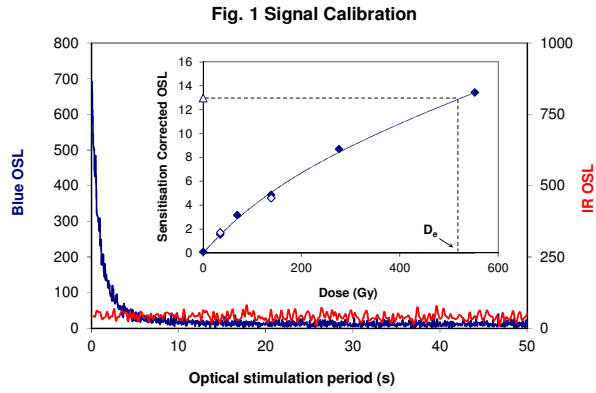## Fig. 6 Signal Analysis

Fig. 7 U Decay Activity

Fig. 8 Age Range

Fig. 1 Signal Calibration Natural blue and laboratory-induced infrared (IR) OSL signals. Detectable IR signal decays are diagnostic of feldspar contamination. Inset, the natural blue OSL signal (open triangle) of each aliquot is calibrated against known laboratory doses to yield equivalent dose (D_e) values. Repeats of low and high doses (open diamonds) illustrate the success of sensitivity correction.
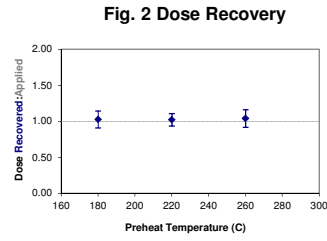
Fig. 2 Dose Recovery The acquisition of D_e values is necessarily predicated upon thermal treatment of aliquots succeeding environmental and laboratory irradiation. The Dose Recovery test quantifies the combined effects of thermal transfer and sensitisation on the natural signal using a precise lab dose to simulate natural dose. Based on this an appropriate thermal treatment is selected to generate the final D_e value.
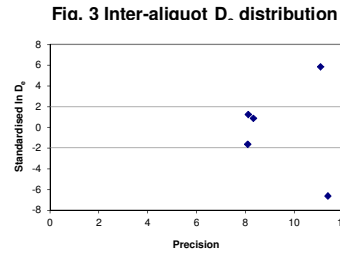
Fig. 3 Inter-aliquot D_e distribution Provides a measure of inter-aliquot statistical concordance in D_e values derived from **natural** irradiation. Discordant data (those points lying beyond ±2 standardised ln D_e) reflects heterogeneous dose absorption and/or inaccuracies in calibration.

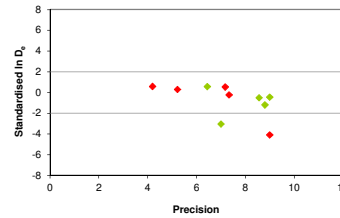**Fig. 4 Low and High Repeat Regenerative-dose Ratio** Measures the statistical concordance of signals from repeated **low** and **high** regenerative-doses. Discordant data (those points lying beyond ±2 standardised ln D_e) indicate inaccurate sensitivity correction.
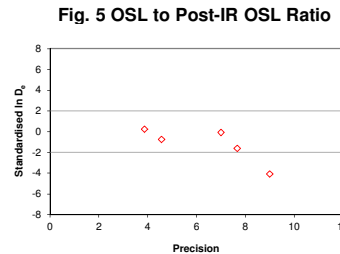
Fig. 5 OSL to Post-IR OSL Ratio Measures the statistical concordance of OSL and post-IR OSL responses to the same regenerative-dose. Discordant, underestimating data (those points lying below -2 standardised ln D_e) highlight the presence of significant feldspar contamination.

Fig. 6 Signal Analysis Statistically significant increase in **natural** D_e value with signal stimulation period is indicative of a partially-bleached signal, provided a significant increase in D_e results from **simulated partial bleaching** followed by insignificant adjustment in D_e for simulated **zero** and **full bleach** conditions. Ages from such samples are considered maximum estimates. In the absence of a significant rise in D_e with stimulation time, simulated partial bleaching and zero/full bleach tests are not assessed.
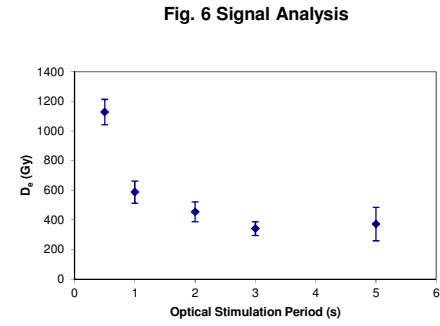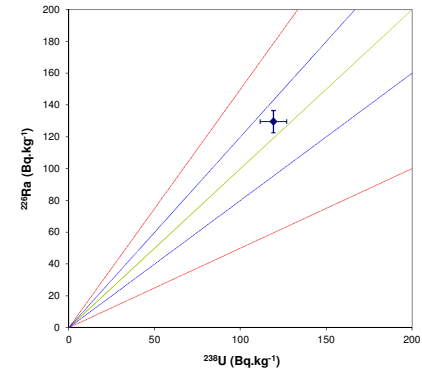
Fig. 7 U Activity Statistical concordance (equilibrium) in the activities of the daughter radioisotope ^{226}Ra with its parent ^{238}U may signify the temporal stability of D_r emissions from these chains. Significant differences (disequilibrium; >50%) in activity indicate addition or removal of isotopes creating a time-dependent shift in D_r values and increased uncertainty in the accuracy of age estimates. A 20% disequilibrium marker is also shown.
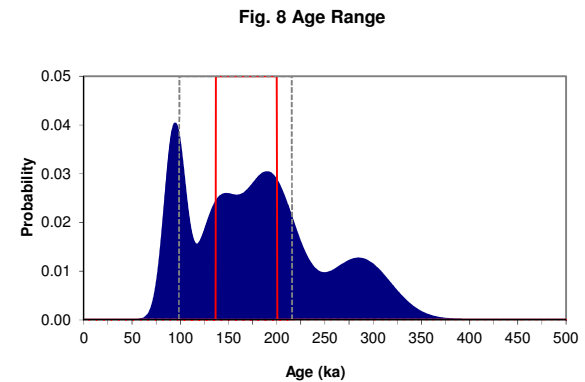
Fig. 8 Age Range The **mean age range** provides an estimate of sediment burial period based on mean D_e and D_r values with associated analytical uncertainties. The probability distribution indicates the inter-aliquot variability in age. The maximum influence of temporal variations in D_r forced by minima-maxima variation in moisture content and overburden thickness may prove instructive where there is uncertainty in these parameters, however the combined extremes represented should not be construed as preferred age estimates.

Sample: GL11023

References

Adamiec, G. and Aitken, M.J. (1998) Dose-rate conversion factors: new data. *Ancient TL*, 16, 37-50.

Agersnap-Larsen, N., Bulur, E., Bøtter-Jensen, L. and McKeever, S.W.S. (2000) Use of the LM-OSL technique for the detection of partial bleaching in quartz. *Radiation Measurements*, 32, 419-425.

Aitken, M. J. (1998) An introduction to optical dating: the dating of Quaternary sediments by the use of photon-stimulated luminescence. Oxford University Press.

Bailey, R.M., Singarayer, J.S. , Ward, S. and Stokes, S. (2003) Identification of partial resetting using D_e as a function of illumination time. *Radiation Measurements*, 37, 511-518.

Banerjee, D., Murray, A.S., Bøtter-Jensen, L. and Lang, A. (2001) Equivalent dose estimation using a single aliquot of polymineral fine grains. *Radiation Measurements*, 33, 73-94.

Bateman, M.D., Frederick, C.D., Jaiswal, M.K., Singhvi, A.K. (2003) Investigations into the potential effects of pedoturbation on luminescence dating. *Quaternary Science Reviews*, 22, 1169-1176.

Berger, G.W. (2003). Luminescence chronology of late Pleistocene loess-paleosol and tephra sequences near Fairbanks, Alaska. *Quaternary Research*, 60, 70-83.

Berger, G.W., Mulhern, P.J. and Huntley, D.J. (1980). Isolation of silt-sized quartz from sediments. *Ancient TL*, 11, 147-152.

Bøtter-Jensen, L., Mejdahl, V. and Murray, A.S. (1999) New light on OSL. *Quaternary Science Reviews*, 18, 303-310.

Bøtter-Jensen, L., McKeever, S.W.S. and Wintle, A.G. (2003) Optically Stimulated Luminescence Dosimetry. Elsevier, Amsterdam.

Duller, G.A.T (2003) Distinguishing quartz and feldspar in single grain luminescence measurements. *Radiation Measurements*, 37, 161-165.

Galbraith, R, F. (1990) The radial plot: graphical assessment of spread in ages. *Nuclear Tracks and Radiation Measurements*, 17, 207-214.

Galbraith, R. F., Roberts, R. G., Laslett, G. M., Yoshida, H. and Olley, J. M. (1999) Optical dating of single and multiple grains of quartz from Jinmium rock shelter (northern Australia): Part I, Experimental design and statistical models. *Archaeometry*, 41, 339-364.

Hubble, J. H. (1982) Photon mass attenuation and energy-absorption coefficients from 1keV to 20MeV. *International Journal of Applied Radioisotopes*, 33, 1269-1290.

Huntley, D.J., Godfrey-Smith, D.I. and Thewalt, M.L.W. (1985) Optical dating of sediments. *Nature*, 313, 105-107.

Hütt, G., Jaek, I. and Tchonka, J. (1988) Optical dating: K-feldspars optical response stimulation spectra. *Quaternary Science Reviews*, 7, 381-386.

Jackson, M.L., Sayin, M. and Clayton, R.N. (1976). Hexafluorosilicic acid regent modification for quartz isolation. *Soil Science Society of America Journal*, 40, 958-960.

Markey, B.G., Bøtter-Jensen, L., and Duller, G.A.T. (1997) A new flexible system for measuring thermally and optically stimulated luminescence. *Radiation Measurements*, 27, 83-89.

Mejdahl, V. (1979) Thermoluminescence dating: beta-dose attenuation in quartz grains. *Archaeometry*, 21, 61-72.

Murray, A.S. and Olley, J.M. (2002) Precision and accuracy in the Optically Stimulated Luminescence dating of sedimentary quartz: a status review. *Geochronometria*, 21, 1-16.

Murray, A.S. and Wintle, A.G. (2000) Luminescence dating of quartz using an improved single-aliquot regenerative-dose protocol. *Radiation Measurements*, 32, 57-73.

Murray, A.S. and Wintle, A.G. (2003) The single aliquot regenerative dose protocol: potential for improvements in reliability. *Radiation Measurements*, 37, 377-381.

Murray, A.S., Olley, J.M. and Caitcheon, G.G. (1995) Measurement of equivalent doses in quartz from contemporary water-lain sediments using optically stimulated luminescence. *Quaternary Science Reviews*, 14, 365-371.

Murray, A.S., Wintle, A.G., and Wallinga, J. (2002) Dose estimation using quartz OSL in the non-linear region of the growth curve. *Radiation Protection Dosimetry*, 101, 371-374.

Olley, J.M., Murray, A.S. and Roberts, R.G. (1996) The effects of disequilibria in the Uranium and Thorium decay chains on burial dose rates in fluvial sediments. *Quaternary Science Reviews*, 15, 751-760.

Olley, J.M., Caitcheon, G.G. and Murray, A.S. (1998) The distribution of apparent dose as determined by optically stimulated luminescence in small aliquots of fluvial quartz: implications for dating young sediments. *Quaternary Science Reviews*, 17, 1033-1040.

Olley, J.M., Caitcheon, G.G. and Roberts R.G. (1999) The origin of dose distributions in fluvial sediments, and the prospect of dating single grains from fluvial deposits using -optically stimulated luminescence. *Radiation Measurements,* 30**,** 207-217.

Olley, J.M., Pietsch, T. and Roberts, R.G. (2004) Optical dating of Holocene sediments from a variety of geomorphic settings using single grains of quartz. *Geomorphology*, 60, 337-358.

Pawley, S.M., Toms, P.S., Armitage, S.J., Rose, J. (2010) Quartz luminescence dating of Anglian Stage fluvial sediments: Comparison of SAR age estimates to the terrace chronology of the Middle Thames valley, UK. *Quaternary Geochronology*, 5, 569-582.

Prescott, J.R. and Hutton, J.T. (1994) Cosmic ray contributions to dose rates for luminescence and ESR dating: large depths and long-term time variations. *Radiation Measurements*, 23, 497-500.

Singhvi, A.K., Bluszcz, A.., Bateman, M.D., Someshwar Rao, M. (2001). Luminescence dating of loess-palaeosol sequences and coversands: methodological aspects and palaeoclimatic implications. *Earth Science Reviews*, 54, 193-211.

Smith, B.W., Rhodes, E.J., Stokes, S., Spooner, N.A. (1990) The optical dating of sediments using quartz. *Radiation Protection Dosimetry*, 34, 75-78.

Spooner, N.A. (1993) The validity of optical dating based on feldspar. Unpublished D.Phil. thesis, Oxford University.

Templer, R.H. (1985) The removal of anomalous fading in zircons. *Nuclear Tracks and Radiation Measurements*, 10, 531-537.

Wallinga, J. (2002) Optically stimulated luminescence dating of fluvial deposits: a review. *Boreas* 31, 303-322.

Wintle, A.G. (1973) Anomalous fading of thermoluminescence in mineral samples. *Nature*, 245, 143-144.

Zimmerman, D. W. (1971) Thermoluminescent dating using fine grains from pottery. *Archaeometry*, 13, 29-52.